Engineering Solid Mechanics 7 (2019) 179-192

Contents lists available at GrowingScience

Engineering Solid Mechanics

homepage: www.GrowingScience.com/esm

A kriging based multi objective gray wolf optimization for hydrazine catalyst bed

M. N. P. Meibody[a], H. Naseh[a*] and F. Ommi[b]

[a]*Aerospace Research Institute, Ministry of Science, Research and Technology, Tehran, Iran*
[b]*Department of Mechanical Engineering, Tarbiat Modares University, Tehran, Iran*

ARTICLEINFO

Article history:
Received 20 December, 2018
Accepted 29 May 2019
Available online
29 May 2019

Keywords:
Multi-objective Optimization
Catalyst bed
Meta-model
Gray Wolf Optimization
Kriging

ABSTRACT

The main aim of this paper is to present a novel multi-objective gray wolf optimization (MOGWO) by utilizing the Kriging meta-model. To this end, surrogate models are used in Multi-Objective Gray Wolf Optimizer as the fitness function. The meta-model is obtained based on exact analysis and numerical simulations. Inheritable Latin Hypercube Design (ILHD) is used as the design of experiments for generation and testing the Kriging model. Then, sensitivity analysis is done to evaluate the effect of design parameter on system responses. The sensitivity analysis leads to appropriate selection of optimization design variables. Hence, the MOGWO algorithm is applied to the problem, the set of non-dominated optimal points are obtained as Pareto Front and one optimal point is selected based on the minimum distance approach. The most important purpose of the methodology is to improve the time consuming in multi-objective optimization problems. In conclusion, for the design of hydrazine catalyst bed was utilized from the proposed methodology. In case, design variables are catalyst bed pellet diameter, loading factor, thrust chamber pressure and Reaction efficiency and objective functions are increasing performance and reducing mass and pressure drop. The results of optimal catalyst bed parameters and also corresponding value of objective functions are shown the performance of methodology in the space propulsion system applications.

1. Introduction

Engineering design is not a single-objective problem. In real problems, the designer usually faces a set of conflicting goals. This multi-objectivity is one of the most important challenges of engineering. On the other hand, the designer is usually trying to reach the optimal answer. Accordingly, the nature of engineering design in real issues is a multi-objective optimization problem (Coello et al., 2007). Unlike single-objective optimization, a set of solutions is the output of the multi-objective optimization process (Branke, 2012). The primary approach in dealing with these problems was the use of mathematical multi-objective optimization techniques. The main disadvantages of these methods were local optima stagnations. In 1984, David Schafer proposed the concept of stochastic optimization based multi-Objective optimization as a revolutionary idea (Deb, 2012). Since then, a significant number of multi-objective heuristic/evolutionary algorithms have been developed(Deb, 2012; Mao-Guo et al., 2009). Strength–Pareto Evolutionary Algorithm (SPEA), Non-dominated Sorting Genetic Algorithm (NSGA),

* Corresponding author.
E-mail addresses: hnaseh@ari.ac.ir (H. Naseh)

doi: 10.5267/j.esm.2019.5.005

Multi-Objective Particle Swarm Optimization (MOPSO), Multi-Objective Evolutionary Algorithm based on Decomposition (MOEA/D), Pareto Archived Evolution Strategy (PAES) and Pareto–frontier Differential Evolution (PDE) are some of well-known stochastic optimization algorithms developed so far (Coello, 2006). Gradient-free mechanism and local optima avoidance are the most prominent characteristics of these methods (Bechikh & Coello, 2018). These characteristics have led to the application of such methods in various engineering fields. According to No Free Lunch (NFL) theorem, which has been logically proved that "**there is no optimization technique for solving all optimization problems**"(Wolpert & Macready, 1997), Efforts to provide new techniques for solving optimization problems are still ongoing. Multi-Objective Grey Wolf Optimizer (MOGWO) is a novel multi objective optimization algorithm proposed by Mirjalili. The social leadership and hunting technique of grey wolves is the main inspiration of MOGWO. The high emphasize on the solutions maintenance and updating mechanism is the main characteristic of this method (Mirjalili et al., 2014; Mirjalili et al., 2016).

Empirical studies and numerical simulations are common approaches to identifying phenomena in engineering sciences. Empirical studies are usually expensive. Therefore, the use of numerical simulations in the design of engineering problems has become commonplace. Numerical simulations are generally time-consuming. This characteristic is the main disadvantage of such methods. So the utilization of a simplified model that could provide an efficient representation of the detailed and costly model is usual during optimization process. As the simplified model is a surrogate for a detailed simulation model it is called a meta-model. The lack of use of meta-model based optimization in literature is obvious.

The purpose of this paper is to provide a comprehensive methodology for design, simulation, sensitivity analysis and Kriging Based MOGWO. Space thruster catalyst bed is selected as the case study. In case, three objectives (increasing performance and reducing mass and pressure drop) are considered as the catalyst bed optimization criteria.

The paper continues on section 2 which introduces the Kriging meta-model methodology algorithm. Section 3 describes the case study. Section 4 presents the results and verification process. Finally, the conclusions are drawn.

2. Kriging Meta-model Methodology Algorithm

In this study, the approach of using Kriging meta-model methodology in the multi-objective Gray Wolf Optimization problems is developed. The MOGWO based on Kriging meta-model methodology is shown in Fig. 1. In this methodology, the first process (left side algorithm) is concerned to the Kriging meta-model generation and the second process (right side algorithm) is performed the multi-objective optimization. To this end, the output of first process (Kriging meta-model) is transferred to second process (multi-objective optimization process). A more explanation of the methodology is presented in the following subsections.

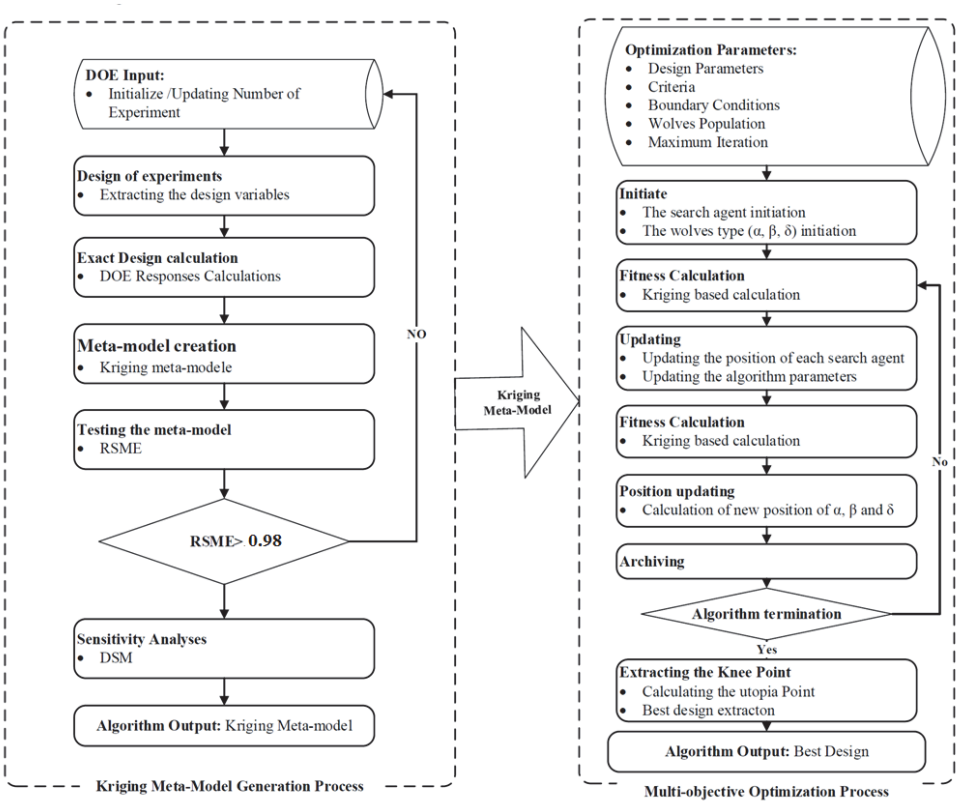

Fig. 1. Kriging Meta-model methodology algorithm

2.1 Meta-model Creation

The exact model applied in the multi-objective optimization can lead to high time-consuming processes. Hence, using surrogate modeling in the optimization process will reduce the calculation effort (Eisenhower et al., 2012). Thus, Kriging meta-model is used in for developing the surrogate model. The procedure is arranged as following steps.

- The DOE is built by Inheritable Latin Hypercube Design (ILHD).
- Based on the design parameters in each experiment, an exact analysis is performed and the system responses are developed.
- About 20% of the samples are randomly selected as test points and used as inputs for surrogate modeling.
- The surrogate model is generated based on Kriging meta-model.
- The response of the system is predicted base on meta-model to test data.
- Root Mean Squared Error (RMSE) is calculated by comparing the meta-model with exact outputs.
- For the RMSE less than 98%, a new design experiments is built by increasing the number of populations up to 50%. This procedure will be continued until the condition of meta-model creation satisfied.
- A sensitivity analysis is performed by the final responses of the DOE.

2.2 Design of experiment

In statistical sensitivity analysis methods and Kriging meta-model development processes, a statistical population is required. This statistical population may be derived from empirical or simulations results. In this study, the required statistical population was developed by using DOE and the results of numerical

simulation. The most DOE methods are Taguchi, Randomized Complete Block Design (RCBD), Latin Square (LS), full factorial (FF), Box–Behnken (BB), Plackett-Burman (PB), central composite (CC), and Latin Hypercube Design (LHD) (Bezerra et al., 2008; Yondo et al., 2017). These methods differ from each other with respect to their characteristics, such as selected points, number of levels for variables, and number of runs. Among the mentioned methods, LHD-based DOEs are especially well suited for Kriging. An inheritable LHD for adaptive Kriging meta-modeling was used in this study. Samples were repetitively generated by fitting a Kriging meta-model in a reduced space (Wang, 2003; Krejci et al., 2011). Identification of design parameters and design criterion has an important role to achieve a suitable DOE. Also, sensitivity analysis can be used as an approach to verify the selection of design parameters and design objectives.

2.3 Kriging Meta-model

Design of meta-models is based on approximations of the exact analysis that are more efficient in calculation and yield insight into the functional relationship between design parameter (x) and the objective functions (y). The use of Kriging is utilized in this paper which has become popular for meta-modeling of time consuming simulations in recent years (Jia & Taflanidis, 2013; Raza & Kim, 2008; Venturelli & Benini, 2016). Kriging meta-model converts the deterministic problem into a statistical framework by combing the global model with a local deviation(Kwon & Choi, 2015). Kriging model interpolates the n_s sampled data points as follow.

$$y(x) = f(x) + \varepsilon(x), \tag{1}$$

where f is known function of x. ε is also stochastic process realization with mean zero, variance σ^2 and non-zero covariance. The covariance matrix of ε is defined as Eq. (2).

$$\mathrm{Cov}\left(\varepsilon(x_i), \varepsilon(x_j)\right) = \sigma^2 \mathbf{R}\left[R(x_i, x_j)\right], \tag{2}$$

where R is the correlation matrix which is a $(n_s \times n_s)$ symmetric matrix with ones along the diagonal. In Eq. 2, $R(x_i, x_j)$ is the correlation function between any two of the n_s sampled data points x_i and x_j. One of the most popular correlation function which has been used frequently in references (Martin & Simpson, 2002; Simpson et al., 2001) is as bellow.

$$R(x_i, x_j) = \sum_{k=1}^{n_{dv}} \theta_k \left| x_i^k - x_j^k \right|^2 \tag{3}$$

where n_{dv} and θ are the number of design variables and the unknown correlation parameters used to fit the model, respectively and x_i^k and x_j^k are the k^{th} components of sampled data points x_i and x_j.

The computation of predicted estimations, $\hat{y}(x)$ of the response $y(x)$ at untried values of x is obtained from Eq. (4).

$$\hat{y}(x) = \hat{\beta} + r^T(x) R^{-1} (y - f\hat{\beta}), \tag{4}$$

where $y_{n\times 1}$ is filled with the sample values of the response and $r(x)_{1\times ns}$ is the correlation vector between an untried x and sampled data points, which can be calculated by Eq. (5).

$$r^T(x) = \left[R(x, x_1), R(x, x_2), \ldots, R(x, x_{n_s})\right]^T. \tag{5}$$

Finally the unknown parameter in Eq. (11), $\hat{\beta}$, is estimated using Eq. (6).

$$\hat{\beta} = (f^T R^{-1} f)^{-1} f^T R^{-1} y \tag{6}$$

The stochastic process realization variance, σ^2, can be estimated from the underlying global model, Eq. (7).

$$\sigma^2 = \frac{\left(y - f\hat{\beta}\right)^T R^{-1}\left(y - f\hat{\beta}\right)}{n_s}. \tag{7}$$

The maximum likelihood estimates for the θ_k in Eq. 3 used to fit the model are found by the optimization as below.

$$\begin{aligned} &\text{max: } L = -\frac{n_s \ln(\sigma^2) + \ln|R|}{2} \\ &\text{subjected to } \theta > 0\ ;\ \theta \epsilon R^n \end{aligned} \tag{8}$$

2.4 Sensitivity analysis

Different statistical analytical methods are used to evaluate the correlation between input parameters and response. The Pearson product moment correlation coefficient or the linear correlation coefficient is a powerful tool for measuring a linear relationship, strength and the direction, between two variables. The linear correlation coefficient for all pair wise combinations of independent and dependent variables is calculated as $\rho_{ij}$and based on Eq. (9) (Most & Will, 2008).

$$\rho_{ij} = \frac{1}{N-1} \frac{\sum_{k=1}^{N} (\hat{y}^{(k)}(x_i) - \mu_{\hat{y}^k(x_i)})(x_j^{(k)} - \mu_{x_j})}{\sigma_{\hat{y}}(x_i)\sigma_{x_j}}. \tag{9}$$

This relationship is used to calculate the linear correlation coefficients between the least-squares fit of a quadratic regression $\sigma_{\hat{y}}(x_i)$ of the variable x_j on the samples $x_i^{(k)}; x_j^{(k)}$. These values vary based on the type of data being examined. The correlation coefficient above 0.7 generally describes the strong correlation between the two variables. While the correlation is less than 0.3, it generally describes the weak relationship between the two parameters. Normally, all of the linear correlation coefficients obtained from the pair-wise parameter combinations of the function variables are presented in a matrix called the design structure matrix (DSM). DSM is a symmetric matrix in which all the diagonal elements are equal (Eppinger & Browning, 2012).

2.5 Multi-Objective Gray Wolf Optimization

Multi-objective optimization problem is generally defined as follows:

$$\begin{aligned} &min \quad F(x) = [F_1(x), F_2(x), \dots, F_k(x)]^T \\ &subject\ to \quad \begin{cases} g_j(x) \le 0 & ; \quad j = 1,2,\dots,m \\ h_i(x) = 0 & ; \quad i = 1,2,\dots,e \end{cases} \end{aligned} \tag{10}$$

where *F(x)* is objective functions vector. x is the design variables vector. $g_j(x)$ and $h_i(x)$ are the inequality and equality constraints, respectively. Herein, Gray Wolves Optimization (GWO) is used as the optimizer. This method is an ultra-fast optimizer with fast convergence and the ability to avoid interception in local optimizations. This algorithm has been implemented with inspiration from the hierarchical leadership and the hunting method of gray wolves. Archiving the non-dominated Pareto optimal solutions assisted by a leader selection strategy is the method to perform multi-objective optimization by GWO.

3. Case Study

The attractiveness of monopropellant thrusters is based on its operational and structural simplicity. Monopropellant thrusters are usually used to attitude and orbit control of spacecraft. These thrusters use catalytic decomposition to change the propellants chemical energy to thermal energy (Larson et al. 1995; Sutton & Biblarz, 2010). Although Hydrazine (Adami et al., 2015a; Jung et al., 2013; Rath et al., 1996; Schmuland et al., 2011), hydrogen peroxide (Adami et al., 2015b; Amrousse et al., 2011; Rhee et al., 2000; Pasini et al., 2011; Whitehead, 1998), Hydroxyl Ammonium Nitrate (HAN) (Chen et al., 2016), De-Methyl Amino Ethyl Aside, hydrazinium nitro formate (HNF) and Nitro oxide(Lohner et al. , 2008) are proposed as liquid monopropellant; hydrazine has received a great deal of attention for many years for space applications that require very high reliability (Hwang et al., 2012).

Monopropellant thruster is composed of thruster valve, injector, catalyst bed, nozzle and body. Except the catalyst bed the other ones are the same mono and bipropellant motor, so it's the most important element of a monopropellant thruster system. In the other hand as the catalyst bed controls propellant decomposition, which determines the overall thruster performance, the importance of this item heightens (Hwang et al., 2012). Transition metal and their derivatives have excellent catalytic behavior (Chen et al., 2002). Between these, the traditional hydrazine catalyst is a 20–40 wt% Ir/g-Al2O3 catalyst. The most successful hydrazine decomposition catalyst to date until 1963 is Shell 405. Shell 405 is 32% iridium over support of alumina, which is capable of surviving several hundred cold starts with no significant degradation. As iridium is a rare and noble metal the Ir-based catalyst is very expensive and many effort have been done to achieve an inexpensive, active, stable and readily available catalyst for hydrazine decomposition (Chen et al., 2016).

Hydrazine propellant decomposes to nitrogen and ammonia in vicinity of its catalyst according to Eq (1). Hydrazine decomposition is a volume expansion and exothermic reaction. Hydrazine decomposed immediately as it contact whit its catalyst. As a result, the chamber pressure and temperature rises rapidly. The released energy of this reaction is about 336.3kjol/mol. This process might occur homogeneously and heterogeneously (Makled & Belal, 2009).

$$3N_2H_4 \xrightarrow{Cat} 4NH_3 + N_2 \tag{11}$$

Additionally, ammonia usually dissociate to nitrogen and hydrogen at elevated temperatures According to Eq (2). Ammonia decomposition is an endothermic reaction and its absorption energy is about 144.5kjol/mol.

$$4NH_3 \xrightarrow{Cat} 2N_2 + 6H_2 \tag{12}$$

So the hydrazine decomposition in a reaction chamber can be simplified as Eq3. where Ψ is ammonia dissociation ratio. That is influenced by on the catalyst type and geometry, the catalyst chamber pressure, and the propellant dwell time.

$$3N_2H_4 \xrightarrow{Cat} 4(1-\psi)NH_3 + (1+2\psi)N_2 + 6\psi H_2 \tag{13}$$

As a result the hydrazine decomposition products properties, molecular weight, specific heat ratio and their temperature depend on hydrazine decomposition and ammonia dissociation proceeding. Hydrazine decomposition will increase the product temperature by releasing thermal energy. In the other hand ammonia decomposition will decrease products temperature and molecular weight. It can be seen in Fig. 2. Hydrazine decomposition products temperature, specific heat ratio and molecular weight falls, increases and decreases respectively as the ammonia dissociation rise.

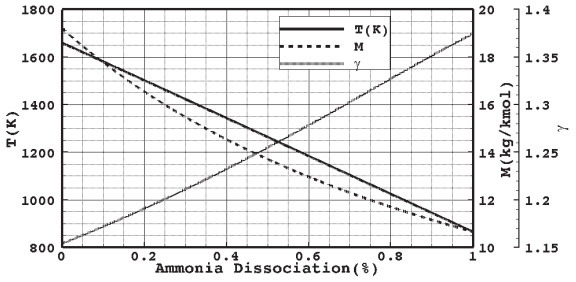

Fig. 2. The hydrazine decomposition products property changes as a function of Ammonia dissociation

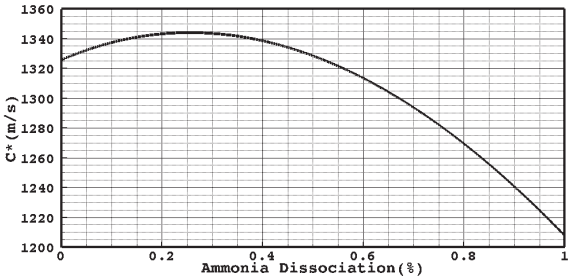

Fig. 3. Hydrazine decomposition products specific velocity changes as a function of ammonia dissociation

Hydrazine decomposition resultant specific velocity changes as a function of ammonia dissociation is illustrated in Fig. 3. The best specific velocity and specific impulse is attained when little ammonia, about %20, is allowed to dissociate.

3.1 Modeling

A one-dimensional decomposition model was developed to calculate reactants temperature and concentration changes through the catalyst bed. A two-step reaction is proposed for hydrazine decomposition. In this model, hydrazine first decomposes into ammonia and nitrogen, and then ammonia dissociates into nitrogen and hydrogen. However, hydrazine decomposition is carried out both in Heterogonous and Homogenous mechanism, but ammonia decomposes only in a catalytic one. Arrhenius reaction model, Eq. (14), was applied for both reactions. According to the first order Arrhenius kinetic equations, the reaction rate ($\dot{r}$) is defined as the product of kinetic rate constant (k) at the species concentration (C_i). The kinetic rate constant, Eq. (15), is defined as the exponential function of activation energy (Ea), reaction temperature (T) and pre-exponential factor (A). The activation energy and the pre-exponential factor used for the modeling of hydrazine and ammonia decompositions are presented in Table 1.

$$\dot{r_i} = k_i C_i \tag{14}$$

$$k_i = A_i \exp\left(-\frac{E_{a_i}}{RT}\right) \tag{15}$$

Table 1. The pre-exponential factor and activation energy of Arrhenius model

Reactant	Reaction	A	E_a
N_2H_4	Catalytic or heterogeneous decomposition	1.50 e+4	2777.78
N_2H_4	Thermal or homogeneous decomposition	2.14 e+10	18333 33
NH_3	Catalytic decomposition	2.53 e+10	27777.78

Activation energy is only a function of the reaction nature and the catalyst type used in the reaction. In other words, activation energy does not affect the geometry and reaction conditions. Since hydrazine is more unstable than ammonia, its dissociation activation energy is far less than the activation energy of ammonia decomposition. Hence, hydrazine decomposition kinetics controls the entire catalytic process of thruster reaction chamber. The pre-exponential factor acts like a scale factor and its unit is sec-1. The pre-exponential factor, in contrast to activation energy, in addition to catalyst type is a function of catalyst bed geometry and reaction conditions. In this study, the catalytic reaction is assumed to be fast enough so that the hydrazine decomposition is performed only on the surface of the particles. The hydrazine decomposition through the particle porosity is neglected.

In a catalyst bed with a porosity ε composed of catalytic particles with an equivalent diameter d_P, the mass ratios of the reactants y_i across the bed can be calculated from Eqs. 16 to 19.

$$\frac{dy_{N_2H_4}}{dx} = \frac{1}{G}\left\{-\varepsilon \dot{r}^{hem}_{N_2H_4} - A_P(K_C C)_{N_2H_4} - \dot{m}\left(\frac{C}{\rho}\right)_{N_2H_4}\right\} \quad (16)$$

$$\frac{dy_{NH_3}}{dx} = \frac{1}{G}\left\{\frac{y_{NH_3}}{y_{N_2H_4}}\left(\varepsilon \dot{r}^{hem}_{N_2H_4} - A_P(K_C C)_{N_2H_4}\right) - A_P\left(K_C\left(C - C_{p_s}\right)\right)_{NH_3} - \dot{m}\left(\frac{C}{\rho}\right)_{NH_3}\right\} \quad (17)$$

$$\frac{dy_{N_2}}{dx} = \frac{1}{G}\left\{\frac{1}{2}\left(\frac{y_{N_2}}{y_{N_2H_4}}\left(\varepsilon \dot{r}^{hem}_{N_2H_4} - A_P(K_C C)_{N_2H_4}\right) - \frac{y_{N_2}}{y_{NH_3}} A_P\left(K_C\left(C - C_{p_s}\right)\right)_{NH_3}\right) - \dot{m}\left(\frac{C}{\rho}\right)_{N_2}\right\} \quad (18)$$

$$\frac{dy_{H_2}}{dx} = \frac{1}{G}\left\{\frac{1}{2}\left(\frac{y_{H_2}}{y_{N_2H_4}}\left(\varepsilon \dot{r}^{hem}_{N_2H_4} - A_P(K_C C)_{N_2H_4}\right) - 3\frac{y_{H_2}}{y_{NH_3}} A_P\left(K_C\left(C - C_{p_s}\right)\right)_{NH_3}\right) - \dot{m}\left(\frac{C}{\rho}\right)_{N_2}\right\} \quad (19)$$

$\dot{m}$ and G are the propellant mass flow rate and propellant loading factor trough the catalyst bed, respectively. A_P is the catalyst bed specific aria per unit volume, which can be calculated from Eq. 20.

$$A_P = \frac{(1-\varepsilon)}{12 d_P} \quad (20)$$

K_{C_i} is the mass transfer coefficient and defined as follows.

$$K_{C_i} = \frac{0.185928 G}{\rho} Sc^{0.667} Re^{-0.41} \quad (21)$$

$$Sc = \frac{\rho D_i}{\mu} \quad (22)$$

$$Re = \frac{G}{\mu A_P} \quad (23)$$

The sepsis e concentration changes can be calculated from Eq. (24).

$$\frac{dC_i}{dx} = \rho \frac{dy_i}{dx} + \frac{C_i}{\rho}\frac{d\rho}{dx}, \quad (24)$$

where ρ is the mixture density. The variation in the mixture density with the assumption of complete gas can be calculated from Eq. (25).

$$\frac{d\rho}{dx} = \rho\left[\frac{1}{P}\frac{dP}{dx} + \frac{1}{\bar{M}}\frac{d\bar{M}}{dx} - \frac{1}{T}\frac{dT}{dx}\right]. \quad (25)$$

$\bar{M}$ is the mixture equivalent molar mass and can be calculated from Eq. (26).

$$\frac{d\bar{M}}{dx} = \bar{M}\frac{\sum_{i=1}^{n}\frac{1}{M_i}\frac{dy_i}{dx}}{\sum_{i=1}^{n}\frac{y_i}{M_i}}. \quad (26$$

Assuming a adiabatic process, the reaction temperature changes can be calculated as the ratio of the enthalpy variations to the mixture specific heat, as presented in Eq. (27).

$$\frac{dT}{dt} = \frac{\sum_{i=1}^{n} -\dot{r}_i h_i}{\sum_{i=1}^{n} -C_i C_{P_i}}. \quad (27)$$

A modified Ergun Equation was used to calculate the catalyst bed pressure drop.

$$\frac{dP}{dx} = \frac{4G}{{d_P}^2 \rho \varepsilon^3}\left(45\mu(1-\varepsilon)^2 + d_P G(1-\varepsilon)\right). \quad (28)$$

Changes in the concentration of ammonia and temperature at each point of the catalyst porous particles can be calculated from the following approximation. K_P is the thermal conductivity of porous catalyst particles.

$$C_{P_{NH3}} = C - \left[\frac{1}{x} - \frac{1}{a}\right]\int_0^x \xi^2 \frac{\dot{r}_{NH_3}^{het}}{D_p} d\xi - \int_x^a \left[\frac{1}{\xi} - \frac{1}{a}\right]\xi^2 \frac{\dot{r}_{NH_3}^{het}}{D_p} d\xi , \quad (29)$$

$$T_P - (T_P)_s = -\left(\frac{H_{NH_3} D_{P_{NH_3}}}{K_P}\right)\left[C_{P_S} - C_p\right]_{NH_3} . \quad (30)$$

A Runge–Kutta Fehlberg method with variable time step is used to calculate the presented differential equations.

3.2 Design Parameter and Design criteria

Reaction chamber pressure, catalyst pellet diameter, catalyst bed loading factor and reaction efficiency are considered as the catalyst bed design parameters. The design domain and parameters variations range are exposed in Table .**2**. It is defined by the nozzle design parameters' minimum and maximum limits. Achieving the highest possible efficiency, along with the lowest mass and power consumption, are the most common goals of the designers of space systems (Fazeley et al., 2016). In this study the performance, mass and pressure drop of the catalyst bed are considered as the design objective.

Table .2 Catalyst bed design parameters and simulation domain

Parameter	unit	min	max
pellet diameter (d_p)	(mm)	0.2	2
loading factor (G)	(kg/m^{2}s)	25	400
thrust chamber pressure(P_{cc})	(Bar)	8	20
Reaction efficiency(η_c)	(%)	85	100

4. Results presentation and verification

The Kriging meta-model methodology algorithm in multi-objective gray wolf optimization problem is shown in Fig. 1. The aim of this section is to apply the methodology to the design process of space low thruster (with 22 N thrust).

4.1 Keriging Modeling

The Keriging Modeling was started with a 100 samples DOE and after five iterations, the Kriging model was produced based on 506 samples. Fig. 4 shows the variation of the objective function RMSE as a function of iteration number. As seen in this figure RMSE constraint is satisfied for all the responses of the model. An example of the response surface generated by this meta-modeling is presented in Fig. 5 and Fig. 6.

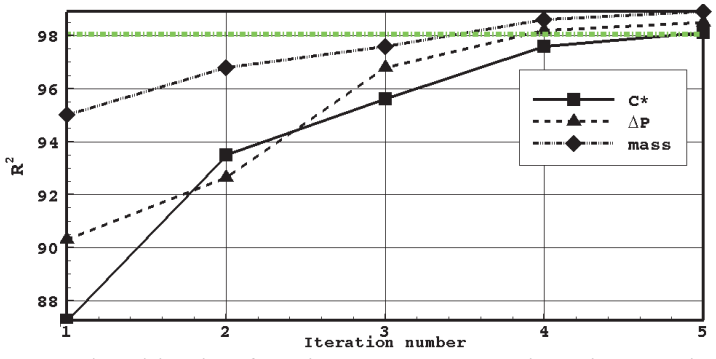

Fig. 4 The objective function RMSE versus iteration number

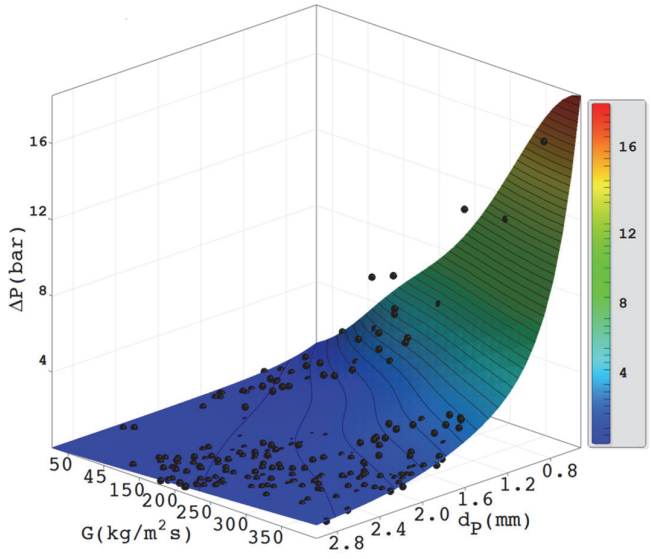

Fig. 5. Response surface of catalyst bed pressure drop with respect to the pellet diameter and loading factor

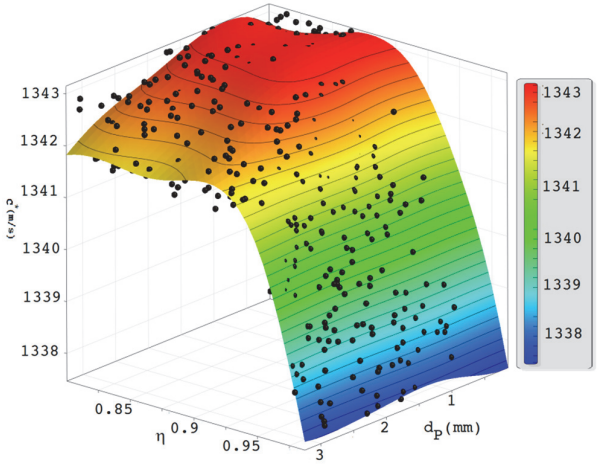

Fig. 6. The specific velocity of catalyst bed products response with respect to reaction efficiency and pellet diameter

4.2 Sensitivity analyses

The catalyst bed sensitivity analysis results are presented in Table 3as a design structure matrix. According to the catalyst bed design structure matrix all design parameters are independent of each other. Also, The DSM shows that the responses are In conflict with each other to each other, which confirms the use of the multi-objective optimal design approach.

Table 3 The design structure matrix of the catalyst bed

	r_p	G	P	η_c	C*	ΔP	m
r_p	1	0	0	0	-0.12	-0.36	0.18
G	0	1	0	0	-0.18	0.56	-0.45
P	0	0	1	0	-0.05	-0.08	-0.18
η_c	0	0	0	1	-0.50	-0.33	-0.45
C*	-0.12	-0.18	-0.05	-0.50	1	0.27	0.31
ΔP	-0.36	0.56	-0.08	-0.33	0.27	1	-0.17
m	0.18	-0.45	-0.18	-0.45	0.31	-0.17	1

4.3 Optimization results

The optimization results of this study are shown as an optimization response called the Pareto front. Pareto front curve or response surface is composed of non-dominated optimization results. Pareto optimal sets allow the designer and decision makers to access a variety of optimal scenarios and choose the one of the best suits the demands of a particular project (Mokarram & Banan, 2017). Monopropellant catalyst bed multi-objective optimization Pareto front is shown in Fig. 7.

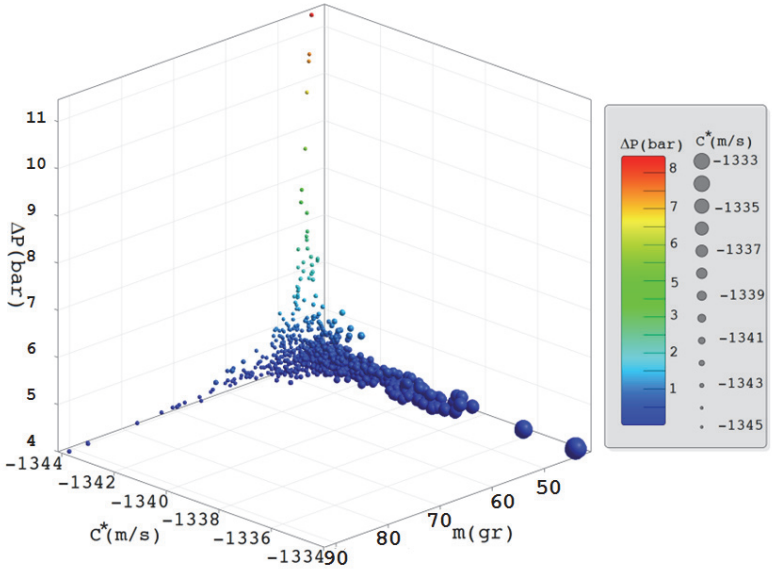

Fig. 7. Multi-objective results (Pareto front) for monopropellant catalyst bed

There are several approaches to find the best solution in the Pareto front. In the paper, minimum distance method is used to choose the appropriate point from the Pareto front. The minimum distance also named knee point method. This point has the minimum distance from the utopia point that is chosen as the appropriate answer. A utopia point is the point which neglected the incompatibility of other objective functions(Branke et al., 2004). An example of how to calculate the knee point is shown in Fig. 8.

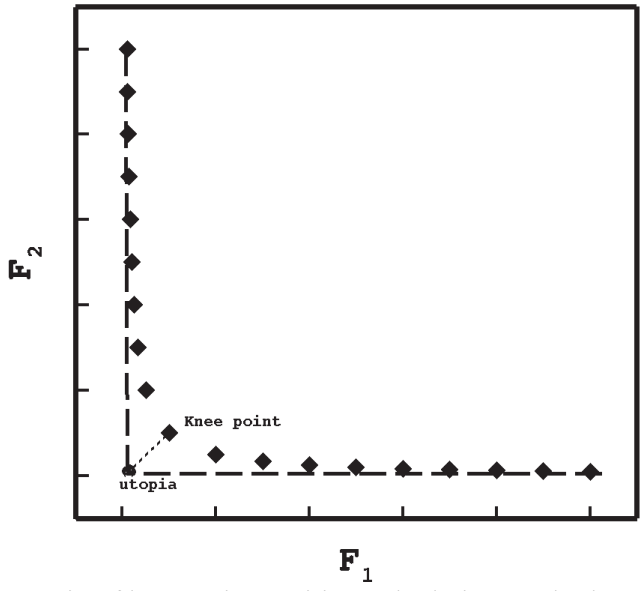

Fig. 8. The schematic of knee point position calculation method on the Pareto front

The results of design variables are compared with the existing thruster's data. This comparison is summarized in Table 4.

Table 4. Comparison of optimization result and existing thruster

Design variables	MR-106E	Proposed methodology
Thrust(N)	22	22
Mass flow(gr/s)	9.4	9.4
Catalyst bed pressure drop (bar)	7.4	6.3
Catalyst bed length(mm)	35	36.5
Catalyst bed diameter(mm)	26	23

5. Conclusions

A novel multi-objective gray wolf optimization assisted by Kriging meta-model is provided in this study. The most important activities in this paper are as follows:

- Meta-model development
- Implementation of The ILHD as the DOE;
- Generation of the Kriging meta-model based on developed model (Fig. 5 and 7);
- Comparing the exact and modeled response of the system by calculation of their RMSE (automatically performed in the algorithm);
- Sensitivity analysis to determine the effect of system parameters (Table 5);
- Applying optimization on the created meta-model
- Applying multi-objective gray wolf optimization and obtaining the Pareto front (Fig. 7);
- Selection of the best design by knee point method (Table 4).

This systematic approach is lead to an accurate, efficient and fast converging multi-objective optimization. The catalyst bed of a hydrazine space low thruster was considered as case study. Three objectives, increasing catalyst bed efficiency and reducing its mass and pressure drop, are considered as the catalyst bed optimization criteria. The proposed approach can be utilized in other engineering optimization problems. The results of this investigation show that, in the Kriging assisted multi-objective grey wolf optimization, CPU time and function calls are lower than using conventional optimization methods. Furthermore, the presented methodology could potentially mitigate some of the difficulties that arise at later stages of the space low thruster design process, and reduce design complexities. In this article, engineering-level analysis codes were used in the conceptual design phase, which can be replaced by high fidelity analysis modules (such as three dimensional CFD or FEA codes) with more capabilities in the detail design phase.

References

Adami, A., Mortazavi, M., Nosratollahi, M., Taheri, M., & Sajadi, J. (2015a). Multidisciplinary design optimization and analysis of hydrazine monopropellant propulsion system. *International Journal of Aerospace Engineering, 2015*.

Adami, A., Mortazavi, M., & Nosratollahi, M. (2015b). Multidisciplinary design optimization of hydrogen peroxide monopropellant propulsion system using GA and SQP. *International Journal of Computer Applications, 113*(9).

Amrousse, R., Brahmi, R., Batonneau, Y., & Kappenstein, C. (2011). *Thermal and catalytic decomposition of H2O2–ionic liquid monopropellant mixtures on monolith-based catalysts.* Paper presented at the Proc. of 46th Joint Propulsion Conference and Exhibit.

Bechikh, S., & Coello, C. A. C. (2018). *Advances in Evolutionary Multi-objective Optimization*. In: Elsevier.

Bezerra, M. A., Santelli, R. E., Oliveira, E. P., Villar, L. S., & Escaleira, L. A. (2008). Response surface methodology (RSM) as a tool for optimization in analytical chemistry. *Talanta, 76*(5), 965-977.

Branke, J. (2012). *Evolutionary optimization in dynamic environments* (Vol. 3): Springer Science & Business Media.

Branke, J., Deb, K., Dierolf, H., & Osswald, M. (2004). *Finding knees in multi-objective optimization.* Paper presented at the PPSN.

Chen, J., Li, G., Zhang, T., Wang, M., & Yu, Y. (2016). Experimental investigation of the catalytic decomposition and combustion characteristics of a non-toxic ammonium dinitramide (ADN)-based monopropellant thruster. *Acta Astronautica, 129*, 367-373.

Chen, X., Zhang, T., Ying, P., Zheng, M., Wu, W., Xia, L., . . . Li, C. (2002). A novel catalyst for hydrazine decomposition: molybdenum carbide supported on γ-Al 2 O 3. *Chemical Communications, 3*, 288-289.

Coello, C. A. C., Lamont, G. B., & Van Veldhuizen, D. A. (2007). *Evolutionary algorithms for solving multi-objective problems* (Vol. 5): Springer.

Coello, C. C. (2006). Evolutionary multi-objective optimization: a historical view of the field. *IEEE Computational Intelligence Magazine, 1*(1), 28-36.

Deb, K. (2012). *Advances in evolutionary multi-objective optimization.* Paper presented at the International Symposium on Search Based Software Engineering.

Eisenhower, B., O'Neill, Z., Narayanan, S., Fonoberov, V. A., & Mezić, I. (2012). A methodology for meta-model based optimization in building energy models. *Energy and Buildings, 47*, 292-301.

Eppinger, S. D., & Browning, T. R. (2012). *Design structure matrix methods and applications*: MIT press.

Fazeley, H. R., Taei, H., Naseh, H., & Mirshams, M. (2016). A multi-objective, multidisciplinary design optimization methodology for the conceptual design of a spacecraft bi-propellant propulsion system. *Structural and Multidisciplinary Optimization, 53*(1), 145-160. doi:10.1007/s00158-015-1304-2

Hwang, C. H., Lee, S. N., Baek, S. W., Han, C. Y., Kim, S. K., & Yu, M. J. (2012). Effects of catalyst bed failure on thermochemical phenomena for a hydrazine monopropellant thruster using Ir/Al2O3 catalysts. *Industrial & Engineering Chemistry Research, 51*(15), 5382-5393.

Jia, G., & Taflanidis, A. A. (2013). Kriging metamodeling for approximation of high-dimensional wave and surge responses in real-time storm/hurricane risk assessment. *Computer Methods in Applied Mechanics and Engineering, 261*, 24-38.

Jung, H., Kim, J. H., & Kim, J. S. (2013). An Approach to the Optimization of Catalyst-bed L/D Configuration in 70 N-class Hydrazine Thruster. *Journal of the Korean Society of Propulsion Engineers, 17*(6), 30-37.

Krejci, D., Woschnak, A., Scharlemann, C., & Ponweiser, K. (2011). Hydrogen peroxide decomposition for micro propulsion: Simulation and experimental verification. *AIAA paper, 5855*, 2011.

Kwon, H., & Choi, S. (2015). A trended Kriging model with R2 indicator and application to design optimization. *Aerospace Science and Technology, 43*, 111-125.

Larson, W. J., Henry, G. N., & Humble, R. W. (1995). *Space propulsion analysis and design*: McGraw-Hill.

Lohner, K., Scherson, Y., Lariviere, B., Cantwell, B., & Kenny, T. (2008). *Nitrous Oxide Monopropellant Gas Generator Development.* Paper presented at the 3rd Spacecraft Propulsion Joint Subcommittee Meeting, JANNAF.

Makled, A., & Belal, H. (2009). *Modeling of hydrazine decomposition for monopropellant thrusters.* Paper presented at the 13th International Conference on Aerospace Sciences & Aviation Technology.

Mao-Guo, G., Li-Cheng, J., Dong-Dong, Y., & Wen-Ping, M. (2009). Evolutionary multi-objective optimization algorithms.

Martin, J., & Simpson, T. (2002). *Use of adaptive metamodeling for design optimization.* Paper presented at the 9th AIAA/ISSMO Symposium on Multidisciplinary Analysis and Optimization.

Mirjalili, S., Mirjalili, S. M., & Lewis, A. (2014). Grey wolf optimizer. *Advances in Engineering Software, 69*, 46-61.

Mirjalili, S., Saremi, S., Mirjalili, S. M., & Coelho, L. d. S. (2016). Multi-objective grey wolf optimizer: a novel algorithm for multi-criterion optimization. *Expert Systems with Applications, 47*, 106-119.

Mokarram, V., & Banan, M. R. (2018). A new PSO-based algorithm for multi-objective optimization with continuous and discrete design variables. *Structural and Multidisciplinary Optimization*, *57*(2), 509-533.

Most, T., & Will, J. (2008). Metamodel of Optimal Prognosis-an automatic approach for variable reduction and optimal metamodel selection. *Proc. Weimarer Optimierungs-und Stochastiktage, 5*, 20-21.

Pasini, A., Torre, L., Romeo, L., Cervone, A., & d'Agostino, L. (2011). Performance Characterization of pellet catalytic beds for hydrogen peroxide monopropellant rockets. *Journal of Propulsion and Power, 27*(2), 428-436.

Rath, M., Schimtz, H., & Steenborg, M. (1996). *Development of a 400 N hydrazine thruster for ESA's atmospheric re-entry demonstrator*. Paper presented at the Proceedings of the 32nd AIAA/ASME/SAE/ASEE Joint Propulsion Conference.

Rhee, M. S., Zakrzwski, C. M., & Thomas, M. A. (2000). Highlights of Nanosatellite Propulsion Development Program at NASA-Goddard Space Flight Center.

Raza, W., & Kim, K.-Y. (2008). Shape optimization of wire-wrapped fuel assembly using Kriging metamodeling technique. *Nuclear Engineering and Design, 238*(6), 1332-1341.

Schmuland, D., Masse, R., & Sota, C. (2011). *Hydrazine propulsion module for CubeSats*.

Simpson, T. W., Poplinski, J., Koch, P. N., & Allen, J. K. (2001). Metamodels for computer-based engineering design: survey and recommendations. *Engineering with Computers, 17*(2), 129-150.

Sutton, G. P., & Biblarz, O. (2010). *Rocket propulsion elements*: John Wiley & Sons.

Venturelli, G., & Benini, E. (2016). Kriging-assisted design optimization of S-shape supersonic compressor cascades. *Aerospace Science and Technology, 58*, 275-297.

Wang, G. G. (2003). Adaptive response surface method using inherited latin hypercube design points. *Journal of Mechanical Design, 125*(2), 210-220.

Whitehead, J. C. (1998). *Hydrogen Peroxide Propulsion for Smaller Satellites*. Paper presented at the 12th Annual AIAA/USU Conference on Small Satellites.

Wolpert, D. H., & Macready, W. G. (1997). No free lunch theorems for optimization. *IEEE transactions on evolutionary computation, 1*(1), 67-82.

Yondo, R., Andrés, E., & Valero, E. (2017). A review on design of experiments and surrogate models in aircraft real-time and many-query aerodynamic analyses. *Progress in Aerospace Sciences*.